Journal of
Marine Science and Engineering

MDPI

Article

Anomalous Oceanic Conditions in the Central and Eastern North Pacific Ocean during the 2014 Hurricane Season and Relationships to Three Major Hurricanes

Victoria L. Ford [1,*,†], Nan D. Walker [1] and Iam-Fei Pun [2]

[1] Department of Oceanography and Coastal Sciences, Coastal Studies Institute Earth Scan Laboratory, Louisiana State University, Baton Rouge, LA 70803, USA
[2] Graduate Institute of Hydrological and Oceanic Sciences, National Central University, Taoyuan 320, Taiwan
* Correspondence: victoriaford@tamu.edu
† Current institution: Climate Science Lab, Department of Geography, Texas A&M University, College Station, TX 77845, USA.

Received: 27 February 2020; Accepted: 14 April 2020; Published: 17 April 2020

Abstract: The 2014 Northeast Pacific hurricane season was highly active, with above-average intensity and frequency events, and a rare landfalling Hawaiian hurricane. We show that the anomalous northern extent of sea surface temperatures and anomalous vertical extent of upper ocean heat content above 26 °C throughout the Northeast and Central Pacific Ocean may have influenced three long-lived tropical cyclones in July and August. Using a variety of satellite-observed and -derived products, we assess genesis conditions, along-track intensity, and basin-wide anomalous upper ocean heat content during Hurricanes Genevieve, Iselle, and Julio. The anomalously northern surface position of the 26 °C isotherm beyond 30° N to the north and east of the Hawaiian Islands in 2014 created very high sea surface temperatures throughout much of the Central Pacific. Analysis of basin-wide mean conditions confirm higher-than-average storm activity during strong positive oceanic thermal anomalies. Positive anomalies of 15–50 kJ cm^{-2} in the along-track upper ocean heat content for these three storms were observed during the intensification phase prior to peak intensity, advocating for greater understanding of the ocean thermal profile during tropical cyclone genesis and development.

Keywords: sea surface temperature; upper ocean heat content; hurricane intensity; Northeast Pacific; Hawaii; Hurricane Genevieve; Hurricane Iselle; Hurricane Julio

1. Introduction

Due to the potentially destructive and deadly nature of powerful tropical cyclones (TCs), a more complete understanding of their genesis and life cycles is imperative. Of the many associated risks, the greatest threats to public health and life are storm surges, flooding, tornadoes, torrential rainfall, and high winds [1]. The 2014 hurricane season in the Northeast Pacific Ocean (NPO) basin was more active than normal. Of the 22 named storms that formed, 16 became hurricanes, and 9 attained major hurricane status (Category 3 and higher; Figure 1). We specifically include Central Pacific TCs in these totals. Long-term averages for the NPO (1981–2010) include 15 tropical storms, 8 hurricanes, and 4 major storms [2]. The NPO accumulated cyclone energy, an index of storm occurrence, duration, and intensity [3], was 162% of the long-term median value [2], indicating that the 2014 NPO season was one of the busiest on record. As a direct result of the 2014 NPO hurricane season, 27 lives were lost and over USD $1.02 billion in damages occurred [2].

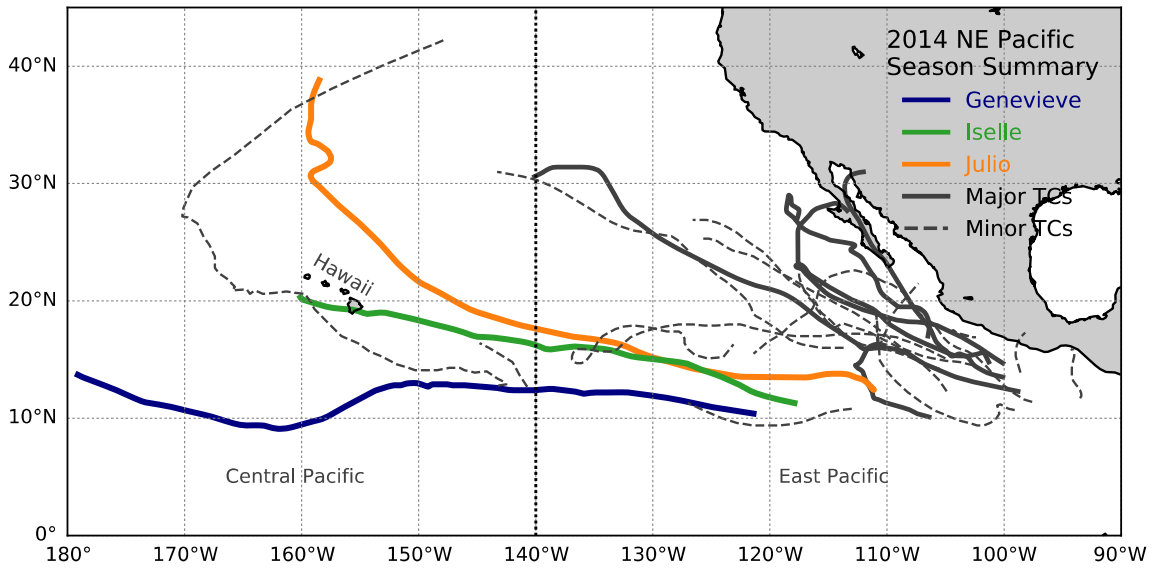

Figure 1. Tropical cyclone (TC) tracks of the 2014 Northeast Pacific hurricane season. Minor TCs (defined as Category 2 status and below) are noted by thin grey dashed line, while major TCs (Category 3 status and above) are in thick grey. TCs of particular interest to our study are highlighted in color—Hurricane Genevieve in blue, Hurricane Iselle in green, and Hurricane Julio in orange. The boundary between the East and Central Pacific basins at 140° W is shown with a vertical gray line.

Of particular interest were the three major TCs that approached the Hawaiian Islands, the third highest occurrence since 1949 [4]. Major hurricane Iselle made a rare landfall on the Island of Hawaii in August 2014 as a strong tropical storm, the first landfall reported there since 1871 [5]. Berg and Kimberlain [6] reported that the Big Island of Hawaii, experienced up to an eight-foot storm surge resulting in week-long power outages and extensive damages to agricultural crops amounting to more than USD $50 million.

TC genesis is influenced by several key atmospheric and oceanic factors; namely, temperature at the surface and extending through sufficient depth in the upper ocean, an initial atmospheric disturbance, a vertical humidity gradient in the lower atmosphere, sufficient Coriolis force, and low vertical wind shear. We specifically focus on the oceanic component of high oceanic temperatures at the sea surface and in the upper ocean involved in generation and maintenance of three NPO TCs in this paper. The required minimum surface temperature to support cyclogenesis is widely agreed to be 26–27 °C [7]. DeMaria and Kaplan [8] and Whitney and Hobgood [9] found that sea surface temperature (SST) acts as an upper limit on the maximum potential intensity of a TC but indicated that other environmental factors also influence the actual intensity of any given TC. Recent oceanic warming has increased tropical SSTs by approximately 0.5 °C between 1970 to 2004, and coincident increases in the number of TCs reaching Category 4 status and higher in the NPO [10].

Perhaps of even greater importance than high SSTs is a sufficiently deep upper ocean thermal structure, which is theorized to energize and intensify tropical cyclones. Leipper and Volgenau [7] coined 'hurricane heat potential' as the excess of heat above 26 °C within the upper ocean. In the tropics, SSTs regularly exceed 26 °C, and thus the depth to which the 26 °C isotherm extends is also vital. Upper ocean heat content (UOHC) and hurricane heat potential [11] are used interchangeably in the literature. For temperatures above this threshold, UOHC provides a vertically integrated estimate of available energy within the upper ocean [12]. The importance of UOHC on intensity changes has been increasingly discussed worldwide (e.g., in the Gulf of Mexico [13]; the North Atlantic Ocean [14]; and the NPO [15]). Lin et al. [16] stressed the criticality of the ocean thermal structure in controlling intensity, especially for the most intense Western NPO storms and those that move slowly. Research on the upper ocean response to a moving TC has also focused on the upwelling and entrainment of

cool, deep waters which lead to a reduction in enthalpy fluxes, the primary energy source for TC maintenance (e.g., [17–20]).

In this study, we analyze the 2014 oceanic conditions during an active hurricane season in the context of sea surface and sub-surface warming across the last decade 2009–2019 in the Eastern and Central NPO. We employ microwave SST observations, UOHC calculations, and their respective anomalies and hypothesize that in addition to high SSTs at genesis, the surface location of the 26 °C isotherm is important for diagnosing the basin-wide surface ocean conditions, as well as maintenance of a high UOHC anomaly. The position of the 26 °C isotherm, both at the surface and at depth, is also believed to be of particular interest as a potential driver of the major hurricane activity in the Central NPO and near the Hawaiian Islands, including a rare landfall on the south coast of the Island of Hawaii.

2. Materials and Methods

2.1. Sea Surface Temperature and Anomalies

This study utilized a wealth of remotely sensed satellite measurements to identify upper ocean thermal structure and anomalous oceanic conditions. The gridded Microwave Optimally Interpolated Sea Surface Temperature version 4 data were obtained from Remote Sensing Systems (REMSS). This dataset blends all data within one day of retrieval from several satellite platforms that have lower frequency channels (6–7 GHz and/or 11 GHz): the Advanced Microwave Sounding Radiometer 2 (AMSR-2), the WindSat radiometer, and the Tropical Rainfall Measuring Mission/Microwave Imager (TRMM/TMI) [21]. Microwave radiometers are especially well suited for observing the sea surface in tropical cyclone environments as the ability to measure SST through clouds is not impeded. Spatial and temporal resolutions are 0.25° and daily, respectively, with an SST measurement accuracy of approximately 0.5 °C [22]. To identify cool wake contamination bias in the SST on TC approach to any particular location, SST values were extracted along-track at daily intervals of 0 to 4 days prior to actual time of hurricane passage [23]. SST '4 days prior' was deemed the most representative of uncontaminated ocean conditions and is used throughout this study (Figure S1). Further notes on SST product quality control are available through REMSS.

National Oceanic and Atmospheric Administration (NOAA) high-resolution SST anomaly version 2 (SSTA) data were provided by the Earth System Research Laboratories Physical Sciences Department (ESRL PSD), which is a high-resolution optimally interpolated blended analysis of SSTs and sea ice concentration from the infrared sensor Advanced Very High Resolution Radiometer (AVHRR) and in-situ ship and buoy observations [24]. Gridded data are available at 0.25° spatial and daily temporal resolutions. The SST monthly anomaly values represent daily observed SST deviations from the long-term 30-year climatological mean covering 1971 to 2000 [25] and highlight the abnormally high ocean temperatures throughout the NPO in our study. We specifically note that the SST and SSTA products used in this study were derived from different remote sensing sensors, each with their own respective inherent biases (see [21,24,25]), and thus exercise caution in discussing the relationship between SST and SSTA products.

2.2. Upper Ocean Heat Content and Anomalies

Upper ocean heat content is a derived variable calculated from satellite microwave SST measurements and contemporaneous satellite altimetry observations. Data for the NPO were derived from a regression model developed first for the Western North Pacific Ocean [26]. The regression method for the Western North Pacific (REGWNP) was developed to improve upon the vertical resolution of the two-layer reduced gravity model (TLM) used in many North Atlantic and NPO oceanic thermal structure studies (e.g., [11,13,15,26]). The TLM calculates upper ocean layer thickness based on the depth of the 20 °C isotherm, in-situ temperature profiles, and AVHRR satellite-retrieved SST [27]. In the REGWNP method, a temperature difference is first calculated between in-situ Argo surface and subsurface temperature profiles, REMSS microwave SST, and the World Ocean Atlas

2001 climatological temperature profiles. The isotherm displacement is linearly regressed onto the corresponding sea surface height anomaly (SSHA) by least squares fit, and varies by location, isotherm, and month. The process is repeated for isotherm depths between 4 and 29 °C. Provided with daily microwave SST, SSHA, and monthly climatological mixed layer depth from the U.S. Naval Research Laboratory, the daily oceanic thermal structure was computed. UOHC was then derived from the oceanic thermal structure profile for the depth of the 26 °C isotherm. The resulting gridded dataset has a spatial resolution of 0.25° and daily temporal resolution. Accuracy estimates of the REGWNP UOHC derivation are discussed in Pun et al. [26]. It is important to note that heat content is a relative quantity where any sub-surface isotherm could be used as a reference. This study used 26 °C as the reference isotherm in determining UOHC values in the NPO. The along-track depths of the 26 °C isotherm during Hurricanes Genevieve, Iselle, and Julio are provided for reference in Figure S2. UOHC anomaly (UOHCA) is the daily UOHC departure [26,28] from the long-term World Ocean Atlas 2013 monthly mean climatological profile covering 1955–2012.

2.3. Tropical Cyclone Observations

We made use of the National Hurricane Center's Hurricane Database 2 (HURDAT2), a best-track post-storm quality-controlled observational record database for the North Atlantic and NPO. Observations from all TCs that attained major hurricane status (wind speeds greater than 50 ms^{-1}) in the 2014 Northeast/North Central Pacific (NE/NC) version of the HURDAT2 were analyzed in Ford [23]. Uncertainty estimates for the North Atlantic best-track parameters are available, and may be applicable to the NPO as well [29]. Latitude, longitude, and maximum wind speed from the NE/NC HURDAT2, as well as SST and UOHC, were spline interpolated to create an hourly observation record for Hurricanes Genevieve, Iselle, and Julio. The interpolation process for the NPO was adapted from the North Atlantic interpolation method found in Elsner and Jagger [30], which preserves values at regular 6 h time intervals, and a piecewise polynomial for values in-between times. For TC location, spline interpolation was determined by spherical geometry. It is noted that the hourly-interpolated data used within are derived, and thus, not best-track quality controlled.

2.4. Methods

Along-track plots of SST, SSTA, UOHC, UOHCA, and corresponding maximum wind speeds (U_Z; ms^{-1}) were investigated. We compared the hourly-interpolated data, the NE/NC HURDAT2 database, and the SST and UOHC datasets for Hurricanes Genevieve, Iselle, and Julio each hour of their duration. Monthly averages of SST, UOHC, and their anomalies illustrate the general oceanic conditions during this time. In this analysis, the 26 °C isotherm was used as the reference threshold from which UOHC was calculated [7].

3. Results

3.1. General Oceanic Conditions

To investigate variability of ocean conditions throughout the NPO in 2014, we present monthly averages of SST, SSTA, UOHC, and UOHCA conditions for July and August as these months included Hurricanes Genevieve, Iselle, and Julio. These three major hurricanes are of specific interest, firstly because they initially formed within an 11-day period at the end of July into early August, and because these three TCs experienced significantly long durations and trajectories into the Central portion of the NPO. Hurricane Hernan, which also formed within the 11-day period, is not discussed here as it was a short-lived minor hurricane that remained within the Eastern NPO.

In July, SST was spatially favorable for TC formation, in excess of 26 °C from the equator to approximately 20–25° N (east of 140° W) and to roughly 30° N (west of 140° W) (Figure 2A). The location of the 26 °C isotherm at the surface is indicated in Figure 2A with a blue dashed line to depict the main area where SST was conducive for TC development and maintenance. In terms of elevated SST,

regions of interest included the western Mexico coastline where SSTs were observed above 30 °C and to the northwest of the Hawaiian Islands, where SSTs in excess of 26 °C extended as far north as 30° N. Hurricanes Genevieve and Iselle (genesis locations shown by star in Figure 2) formed in July in regions of relatively high SSTs of 28.95 °C and 28.65 °C, respectively. Positive SSTAs were widespread across the study area (Figure 2B) and ranged from 0–2 °C throughout the TC generation area, defined as the longitudinal band between 10° to 20° N in the NPO tropics [31]. The maximum observed SSTAs in July were located in the Eastern NPO and exceeded 2 °C across a large region north of 15° N and south of 5° N. (Figure 2B). Iselle's westward trajectory followed the surface location of the 26 °C isotherm closely between 135° and 155° W before striking the Big Island of Hawaii. Genevieve travelled a more southerly path, but also experienced mostly positive SSTAs along its track. A region of weak negative anomaly (0 to −0.5 °C) was observed north of 20° N between 125° and 140° W, and a stronger negative anomaly of up to −2 °C was detected near 40° N near the International Date Line. Between those negative SSTA regions, a strong positive SSTA zonal-oriented band extended from 130° W to 180°, and may be related to the "Blob" generated during the 2013–2014 winter from abnormally low oceanic heat loss, due to abnormally high sea level pressure [32]. Although the "Blob" was centered in the extratropics, it extended southward to 30° N between 125°–150° W. To summarize, the dominant observation regarding SST in July 2014 was that of an anomalously high surface temperature regime throughout the Central and Eastern NPO where TCs formed and tracked during hurricane season.

UOHC in July averaged between 25–35 kJ cm^{-2} across much of the NPO in areas where SSTs exceeded 26 °C (Figure 2C), with regions of higher values centered off the coast of Acapulco, Mexico and extending offshore to the region where Iselle and Genevieve formed. The highest UOHC detected emanated from the Western Pacific Warm Pool into the NPO as far east as 135° W between the equator and 7° N, south of the normal TC generation region. UOHC in this region exceeded 150 kJ cm^{-2}, indicating very high upper ocean temperatures that reached a considerable depth. Although UOHC values northwest of the Hawaiian Islands extended beyond 30° N, values were higher west and southwest of the Islands. At the time of genesis, Genevieve and Iselle experienced 46 kJ cm^{-2} and 61.5 kJ cm^{-2} of UOHC, respectively, well above the basin-wide average. We note that Genevieve made a southerly turn at approximately 155° W towards the higher UOHC tropical region before transitioning into a major hurricane. In Figure 2D, the UOHC anomaly reveals that much of the NPO tropical region experienced a positive UOHC anomaly between 0 to 40 kJ cm^{-2}. The high UOHC region close to the western tropics exceeded 80 kJ cm^{-2} in UOHC anomaly. Although Iselle formed in an area of positive UOHCA, it tracked over lower values of UOHC and near 0 kJ cm^{-2} UOHCA after it reached 125° W. It even tracked over small regions of negative UOHCA (Figure 2C,D). North of the Hawaiian Islands we observed evidence of positive UOHC anomalies ranging from 0 to 10 kJ cm^{-2}, primarily due to the surface expression of the 26 °C isotherm above 30° N.

By August, the surface location of the 26 °C isotherm extended well above the Hawaiian Islands approaching 32–33° N between 150° and 180° W (Figure 3A). Notable around Iselle's trajectory was the northward shift of the 26 °C isotherm at the surface between 140° and 150° W towards 18° N, which was approximately parallel to the southern coastline of the Big Island of Hawaii. SSTs surrounding the Baja Peninsula and western Mexico's coastline increased in value, while the 26 °C isotherm at the surface in the eastern tropics also shifted northward approximately 1°. Hurricane Julio followed close behind Iselle, also following along the surface expression of the 26 °C isotherm, especially to the northeast and north of the Hawaiian Islands. It is notable that Julio transitioned from hurricane status to a tropical storm (thick line to dashed line; Figure 3A) around the terminus of the 26 °C isotherm's northern extent. SST anomaly in August revealed a strengthening of anomalous temperatures in the NPO, especially in a widespread region surrounding the Baja Peninsula and extending southwestward to approximately 140° W. Basin-wide, SST anomalies averaged between 1.0 and 1.5 °C. The high SST anomaly region converging around the Baja Peninsula, coupled with very high SSTs above 30 °C, provided extremely favorable long-term conditions for TC development close to the coast. The high SST anomaly region associated with the "Blob" north of 30° N covered a large swath of ocean between 130° and 150° W

with positive anomalies higher than 2.0 °C, but below 26 °C SST value, which was why there was no indication of the "Blob" in our presently defined UOHC/UOHCA record. While not conducive for TC development and maintenance, anomalously high SSTs in this extratropical area had important fishery implications and regional weather impacts for the western U.S. coastline [32].

An inspection of August UOHC and UOHCA revealed a continuation of an anomalous spatial distribution of the warm surface layer, especially in the Central NPO to the west, north, and south of the Hawaiian Islands (Figure 3C,D). While UOHC values above 20° N averaged around 20 kJ cm^{-2}, the connection to the wide swath of SST anomaly in the extratropics makes a compelling case for a 'warmer-than-average' diagnosis for the Central NPO in 2014 from the equator to 30° N. A smaller, confined loci of high UOHC along the Mexican coastline moved to the southwest compared to July, influencing the area of Julio's generation. South of 10° N, the eastward extension of the West Pacific Warm Pool produced a long tongue-like feature of high UOHC, a feature that was also revealed in the UOHCA patterns (Figure 3C,D). UOHC values approached 200 kJ cm^{-2} within this southerly feature that may have impacted the intensification of Genevieve, as a result of the anomalously deep warm layer. Positive UOHC anomalies (Figure 3D) were observed throughout much of the NPO ranging from 5 to 60 kJ cm^{-2}, with two main regions of higher UOHC anomaly: off the western Mexico coastline and the western extension of high UOHC anomaly in the Central NPO. These two regions each exceeded 70 kJ cm^{-2}. Notable is a region of negative UOHCA at the equator near 146° W of less than −10 kJ cm^{-2} that spatially aligned with a similar pattern in SST and SST anomaly. It is of great interest that although Iselle and Julio formed in areas of high SST, SSTA, UOHC, and UOHCA, they were able to maintain hurricane strength over waters with minimal UOHC and low SST.

To determine how unusual the observed SST and UOHC anomalies were in July and August 2014, we calculated the monthly mean SST and UOHC anomalies across the zonal latitude band between 10–20° N in the NPO over the most recent decade 2009–2019 (Figure 4). The vast majority of TC cyclogenesis occurs in this band for the Eastern NPO [31] and Central NPO [23]. We also show TC counts in July and August for the NPO, broken down by basin—East NPO or Central NPO cyclogenesis locations—and by intensity for those storms above major hurricane status (Category 3 and above on the Saffir–Simpson scale) (Figure 4A). In 2009, the number of July and August TCs in the NPO exceeded 12 storms, with 2 additional TCs originating in the Central NPO. Following this period, TC counts in July and August remained below 6 storms until 2013 when TC counts increased again for a total of 11 storms. In 2014, there were 10 TCs originating in the Eastern NPO, 4 of which attained major hurricane status. A star is denoted in 2014 for Hurricane Iselle, which made a rare landfall on Hawaii. The number of storms increased in July and August of 2015 and 2016. Hurricane Darby made landfall in 2016 on the Island of Hawaii, the second landfalling strike in two years. Following 2016, TC counts in the NPO decreased slightly, ranging between 9 and 11 storms.

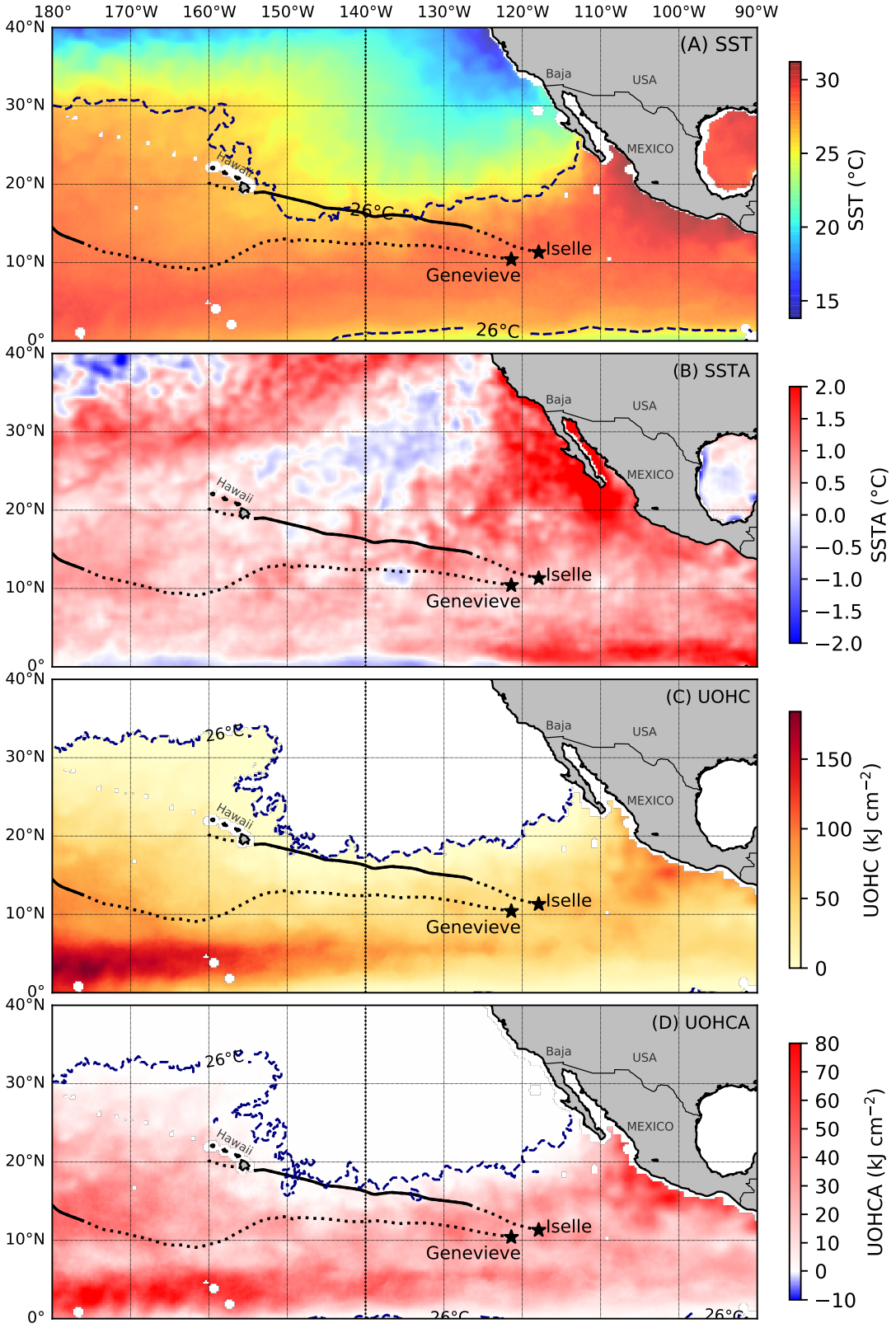

Figure 2. Oceanic conditions and anomalies during July 2014 in the Northeast Pacific Ocean (NPO) as seen in (**A**) sea surface temperature, (**B**) sea surface temperature anomaly, (**C**) upper ocean heat content, and (**D**) upper ocean heat content anomaly. The surface location of the 26 °C isotherm is contoured in blue for reference. The trajectories of Hurricanes Genevieve (25 July–7 August) and Iselle (31 July–9 August) are provided, with a star representing the genesis location. TC trajectory denoted by: black dashed line for tropical storm status (below 33 ms^{-1}) and thick black line for hurricane status (above 33 ms^{-1}).

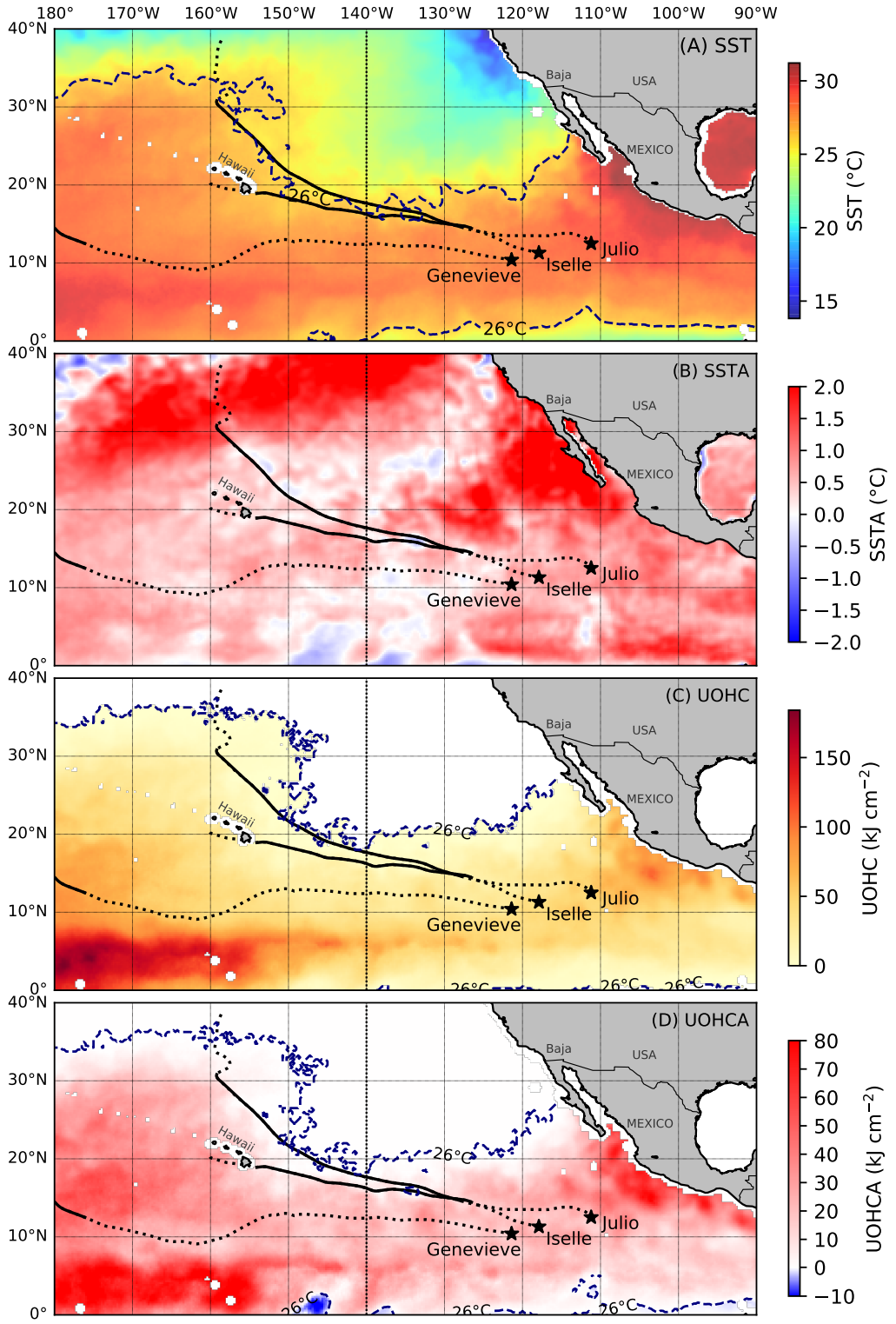

Figure 3. Oceanic conditions and anomalies during August 2014 in the Northeast Pacific Ocean (NPO) as seen in (**A**) sea surface temperature, (**B**) sea surface temperature anomaly, (**C**) upper ocean heat content, and (**D**) upper ocean heat content anomaly. The surface location of the 26°C isotherm is contoured in blue for reference. The trajectories of Hurricanes Genevieve (25 July–7 August), Iselle (31 July–9 August), and Julio (2–18 August) are provided, with a star representing the genesis location. TC trajectory denoted by: black dashed line for tropical storm status (below 33 ms^{-1}) and thick black line for hurricane status (above 33 ms^{-1}).

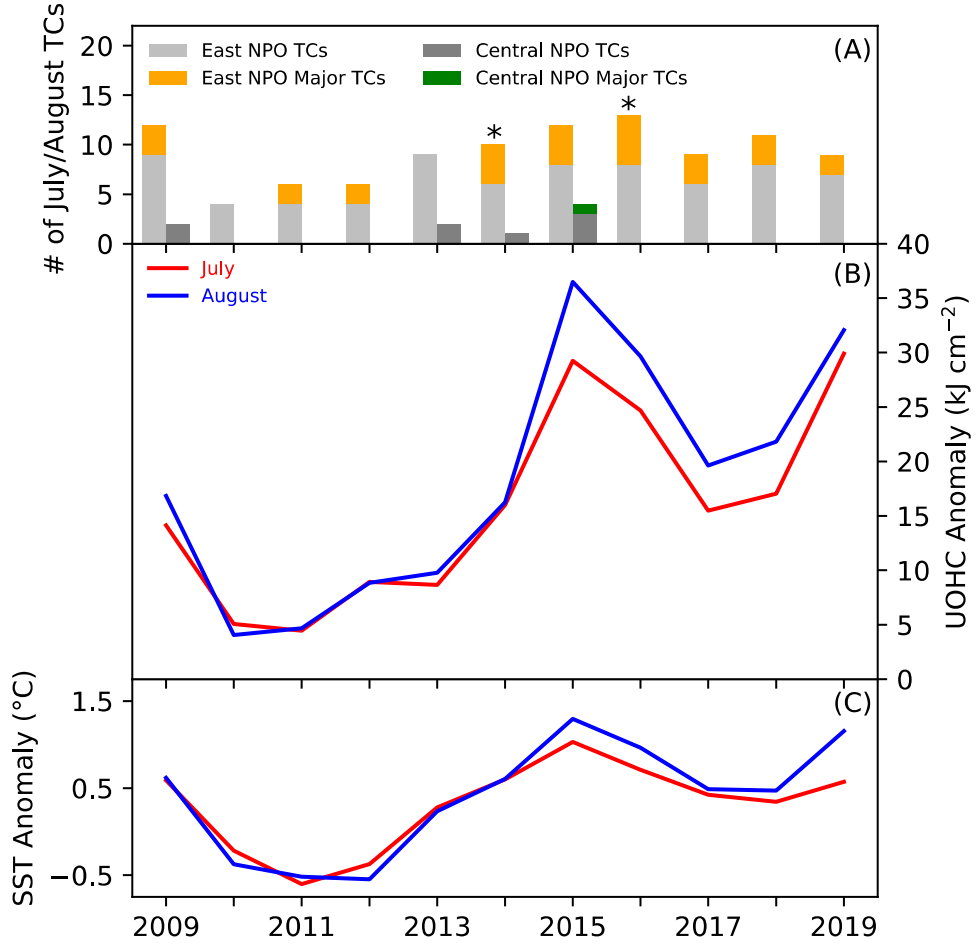

Figure 4. (**A**) July and August TC counts for 2009–2019, broken down by genesis in either the East NPO or the Central NPO, and by minor or major hurricane status. Stars indicate a Hawaiian landfalling TC in this timeframe. July and August monthly mean (**B**) upper ocean heat content (UOHC) anomalies and (**C**) sea surface temperature (SST) anomalies in the 10–20° N NPO cyclogenesis region 2009–2019.

Mean UOHC anomalies in 2009–2019 indicate positive anomalies throughout the cyclogenesis region, ranging from 5–10 kJ cm^{-2} between 2010 and 2013, and as high as 36 kJ cm^{-2} in 2015 (Figure 4B). Mean UOHC anomaly in July and August 2014 was 16 kJ cm^{-2}, which denotes the beginning of the increasing mean anomaly seen in 2015 and onwards. A decrease in UOHCA was also observed between 2017 and 2018 to approximately 15–23 kJ cm^{-2}, before increasing in mean anomaly in 2019. SST anomalies follow much of the same pattern as UOHCA (Figure 4C). A negative SST anomaly was observed between 2010 and 2013 of −0.5 °C, while SST anomalies above 0.5 °C were observed in July and August between 2014 to 2019. We note that the negative SSTA period coincides with weaker UOHCA than the surrounding years. SST anomalies above 1 °C were observed in 2015 and August 2019. In July and August 2014, the mean SST anomaly in this latitude band was 0.60 °C and 0.61 °C respectively. July and August 2009–2019 SSTA and UOHCA patterns closely followed the observed number of TCs during this time. A negative SSTA and UOHCA anomaly below 10 kJ cm^{-2} was seen when TC counts were low between 2010–2013. An increase in TC counts, with two Hawaiian-landfalling TCs, occurred with a strong positive SSTA of greater than 0.5 °C and UOHCA above 15 kJ cm^{-2}. This observation aligns well with the understanding that wintertime positive El Niño events increase the subsurface heat in the NPO, which can intensify NPO TC activity in the following seasons [33]. Based on the Climate Prediction Center Oceanic Nino Index (ONI), the Julys and Augusts of 2009, 2015, and 2019 were above +0.5 °C (associated with positive El Niño phase), and 2010, 2011, and 2016 were below

−0.5 °C (associated with negative La Niña phase). While the active 2014 NPO TC season, and the contemporaneous SST and UOHC anomalies, are considered to be during 'neutral' conditions not tied to a positive El Niño event, the high TC frequency and the spatial distribution of developing oceanic anomalies leading up to the 2015 El Niño event may prove to be a useful example in furthering our understanding of the relationship between TCs and warming oceanic conditions.

3.2. Storm-Specific Oceanic Conditions

3.2.1. Hurricane Genevieve

Hurricane Genevieve was the first in a sequence of four TCs that formed in the NPO over an 11-day period in late July and early August [34]. Genevieve spent most of its lifecycle within the Eastern and Central NPO oscillating between tropical storm and tropical depression status (Figure 5). After tracking west-southwest of the Hawaiian Islands, around 175° W Genevieve underwent rapid intensification and attained hurricane status on 6 August and major hurricane status on 7 August. While still in the Central NPO, Genevieve was a major hurricane for 6 h with 67 ms^{-1} wind speeds minutes before crossing the International Date Line (180°) into the Western NPO basin. Records from the Japanese Meteorological Agency indicated that Genevieve reached 72 ms^{-1} winds quickly [34] within the Western NPO, and was classified as a super-typhoon, the equivalent of a Category 5 hurricane. An extremely rare occurrence, Genevieve existed in all three Pacific Ocean hurricane basins at some instance throughout its entire lifecycle. Based off of the NE/NC HURDAT2 record, this has only occurred seven other times since 1949.

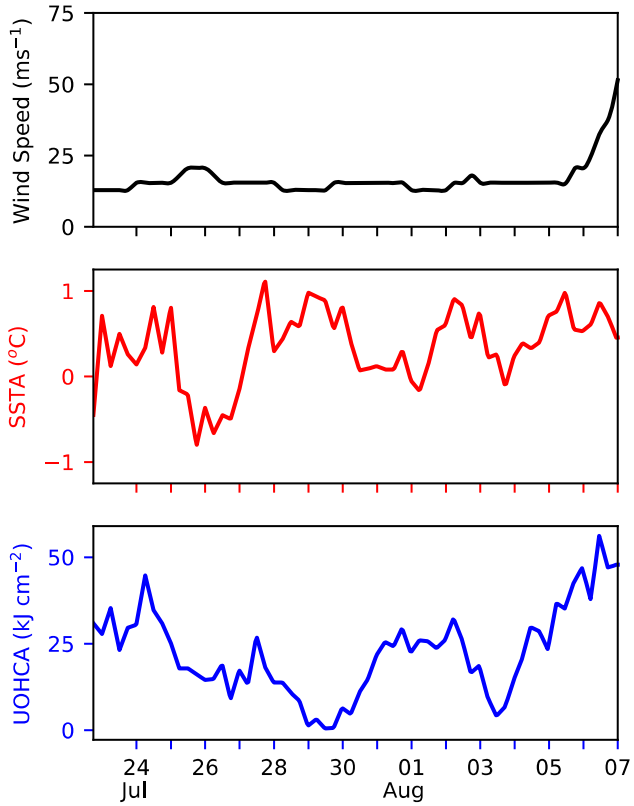

Figure 5. Along-track time series record for Hurricane Genevieve through (**Top**) maximum sustained wind speed with TC intensity category indicated, (**Center**) SST anomaly, and (**Bottom**) UOHC anomaly.

The along-track analysis for Genevieve indicates that despite an extended period of weak TC maintenance, SSTs along its path remained above a positive SST anomaly for most of its duration as a TC in the East and Central NPO basins (Figure 5). Interestingly, SST anomaly at the time of

genesis was found to be slightly negative, at −0.45 °C. SST anomaly along Genevieve's path was largely positive, between 0° and 1 °C, with brief periods of negative SST anomaly, with the largest negative anomaly lasting from 05:00 Coordinated Universal Time (UTC) 25 July to 01:00 UTC 27 July, but never lower than −0.8 °C. Coincidentally, this period also corresponded to Genevieve's brief interlude spent at tropical storm status prior to rapid intensification. Starting at 00:00 UTC on 6 August, Genevieve transitioned from a weak tropical storm towards major hurricane status (50 ms^{-1} and greater). During this time, SST anomaly followed much of the same pattern as previously observed (Figure 5), ranging from a positive 0.5 °C to 0.8 °C SST anomaly, which would likely not account for the rapid change of TC intensity. In this regard, we consider the UOHC anomaly and note that UOHC anomaly along-track remained positive throughout. At genesis, UOHC anomaly was 30.9 kJ cm^{-2}. Throughout Genevieve's duration, UOHC anomaly oscillated between 0 and 35 kJ cm^{-2} until 3 August, when Genevieve subsequently tracked over a region of higher positive UOHC anomaly that steadily increased along-track UOHCA to 56 kJ cm^{-2} near 155° W and westward. Looking back to Figures 2 and 3, we observed that the southwestward turn in Genevieve's track brought the TC to the very northern edge of the West Pacific Warm Pool extension of very high UOHC, but also large positive UOHC anomalies at that time as well. We note that this 72-h period of increasing UOHCA prior to rapid intensification on 6 August may have been an oceanic influence on the development of Genevieve into a major hurricane. Storm conditions, SST, and UOHC for Genevieve's duration in the Western Pacific were not investigated in this study.

3.2.2. Hurricane Iselle

Along-track conditions revealed that Iselle formed as a tropical low and traveled over a consistently high positive SST anomaly of 0.5 to 1.0 °C for 36 h after storm genesis on 30 July (Figure 6). Subsequently, Iselle moved into a region of relatively lower positive SST anomaly, hovering around the 0.0 °C anomaly threshold, indicating normal SST conditions in that region of the NPO at this time. Iselle tracked above two regions on 3 August and 5 August of moderately low negative SST anomaly of up to −1 °C, before transitioning back into an area of slightly higher than average SST conditions (Figure 3). We observed that the SST anomaly had more variation in values during this time, ranging from slightly positive anomaly to a moderate negative anomaly. In regards to the UOHC anomaly, genesis occurred in very high UOHCA conditions of 40 kJ cm^{-2}, the highest value observed throughout Iselle's lifespan (Figure 6). UOHC anomaly then dropped to approximately 15 kJ cm^{-2}, shortly after genesis but then increased steadily to 30 kJ cm^{-2} by 1 August. A similar rise and fall of the UOHC anomaly pattern continued over the next few days, with the overall pattern indicating a gradual decline of UOHC anomaly before values dipped into a minor negative UOHC anomaly late on 3 August, not exceeding −3 kJ cm^{-2}. At the time of peak TC wind speed intensity as a Category 4 hurricane, UOHC anomaly ranged from 13 to 14 kJ cm^{-2}. We note that the presence of a positive, but generally declining UOHC anomaly from time of genesis to peak intensification was present along-track for Iselle. Interestingly, UOHC anomaly appeared to increase slightly shortly before landfall on the Puna Coast of the Big Island of Hawaii on 8 August 12:30 UTC.

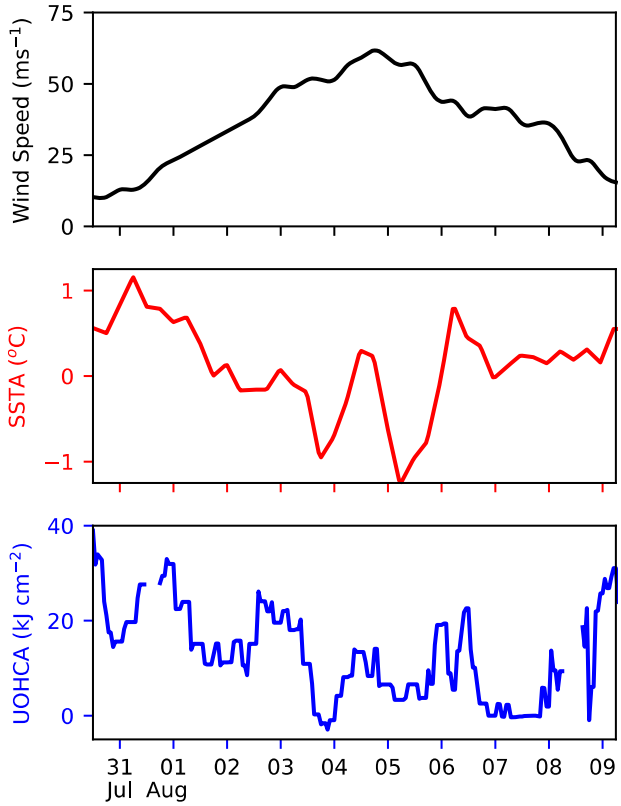

Figure 6. Along-track time series record for Hurricane Iselle through (**Top**) maximum sustained wind speed with TC intensity category indicated, (**Center**) SST anomaly, and (**Bottom**) UOHC anomaly. Landfall is denoted by a break in the UOHC anomaly record. Gap in UOHC anomaly coverage occurred during landfall event.

3.2.3. Hurricane Julio

Time series analysis indicated that Julio formed in a region of slight positive SST anomaly of 0.5 °C (Figure 7), which steadily increased to 1.0 °C before it encountered an oscillating pattern of weak positive to weak negative SST anomalies along-track throughout peak intensity. Julio experienced a weak second increase in TC intensity briefly on 13–14 August. At this time the SST anomaly experienced wide swings between negative anomalies of −0.8 °C and positive anomalies of 1.1 °C. The along-track SST anomaly after this second peak intensity phase then increased to a peak of 2.0 °C, the largest SST anomaly seen along-track for any of the three storms of interest. Figure 3B reveals that this SST anomaly resulted from the large swath of very high SST anomaly throughout the extratropical band north of the Hawaiian Islands in the NPO. Unlike the previous two TCs, Julio's genesis occurred in an area of negative UOHC anomaly of −0.65 kJ cm^{-2} before it quickly increased along-track to a peak of 41 kJ cm^{-2} (Figure 7). UOHC anomaly throughout the first intensification phase for Julio remained positive, averaging between 10 and 20 kJ cm^{-2}. Like Iselle, Julio's peak UOHC anomaly appeared several days prior to peak intensification, with a varying but declining UOHC anomaly afterwards. After Julio reached peak TC intensity as a Category 3 hurricane, along-track UOHC anomaly dropped to near 0 kJ cm^{-2} for approximately 72 h, before entering a region of comparatively low positive UOHC anomaly between 10 to 15 kJ cm^{-2} at the same time as Julio's second increase in intensity to a Category 1 hurricane on 14 August. UOHC anomaly then decreased quickly on 16 August to 0 kJ cm^{-2} for the remainder of storm duration as Julio dissipated. As with Genevieve and Iselle, we noted the importance of positive UOHC anomaly during the intensification phase of Julio prior to reaching peak intensity.

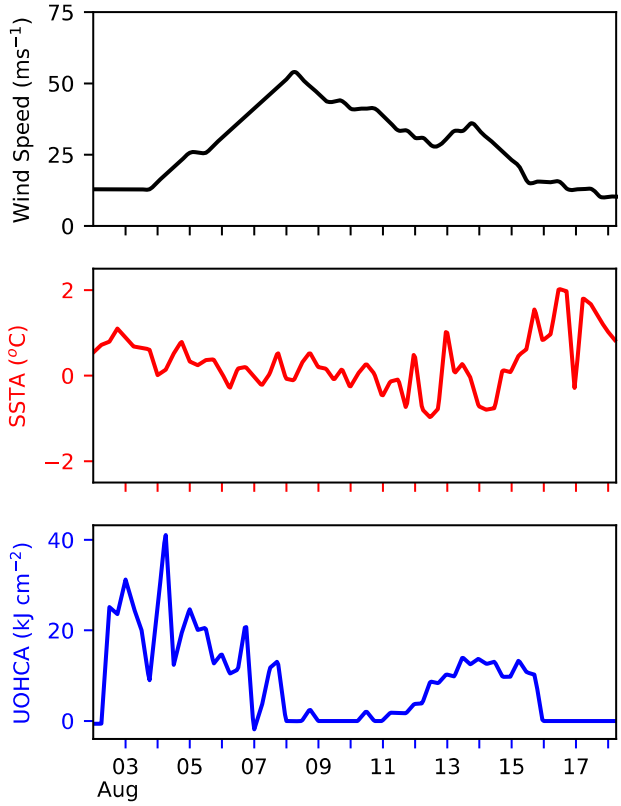

Figure 7. Along-track time series record for Hurricane Julio through (**Top**) maximum stustained wind speed with TC intensity category indicated, (**Center**) SST anomaly, and (**Bottom**) UOHC anomaly. Note: change in scale for SST anomaly (SSTA).

4. Discussion and Conclusions

This research employed SST, SSTA, UOHC, and UOHCA to investigate the anomalous oceanic environment during the generation and mature phases of three major East and Central North Pacific hurricanes in July and August 2014. Basin-wide maps revealed that SST and UOHC were higher than normal over large areas of the Eastern and Central NPO from 0–40° N during the 2014 hurricane season. Maximum SST anomalies occurred along the Mexican coastline and extended offshore to 140° W. The UOHC anomalies in the Eastern NPO did not extend as far north as the SST anomalies but were more spatially concentrated between 5–25° N in the normal generation area for TCs [31]. These anomalous SST and UOHC conditions in the cyclogenesis region between 10–20° N across the NPO may have expanded the area of TCs and hurricane activity to the west and northwest. Hurricane Genevieve formed in the Eastern NPO at 121° W, before crossing the entire breadth of the Central NPO, and reached peak intensity in the Western NPO. Both Hurricanes Iselle and Julio formed in the Eastern NPO before tracking on northwestward paths towards the Hawaiian Islands, including a landfalling strike and an unusual northern trajectory. This was especially true for the region surrounding the Hawaiian Islands and the Central NPO, where maximum positive SST and UOHC anomalies were present north of 30° N into the extratropics. We also make note of the "Blob" present throughout the 2014 hurricane season, where its southern extension is present in the SST/SSTA analyses as a strong +2 °C anomaly.

A few critical observations were made from the along-track analyses. An increase of 50 kJ cm^{-2} in UOHCA was observed prior to and throughout the intensification phase of Genevieve, before tracking into the Western NPO, where further intensification led to the equivalent of a Category 5 hurricane. UOHCA remained high from genesis to peak intensity for both Iselle and Julio, with values typically between 20–30 kJ cm^{-2}. Julio's second brief intensification phase was precluded by an increase in

along-track UOHCA from 0 kJ cm^{-2} up to 13 kJ cm^{-2}. The main inference drawn from each of these case studies was the importance of a positive UOHC anomaly present within the development or intensification phase of each of these storms at least 24 h prior to and up to peak intensity, and in Julio's case, a second brief intensification phase. In both Iselle and Julio's intensification phases from cyclogenesis to peak intensity, we noted that the highest UOHCA was observed some time prior to attaining their respective maximum intensities, with positive but declining UOHC anomalies observed afterwards. There may be a variety of factors leading to and influencing this behavior. The oceanic conditions that we have presented are only one component out of several, including the influence of atmospheric circulation, that are involved in the maintenance and peak intensification of any particular TC. More comprehensive research into the importance of positive SST and UOHC anomalies present throughout genesis, intensification, and peak intensity is needed.

A diagnosis of basin-wide SST and UOHC conditions, and their respective anomalies, pointed towards the importance of the location of the 26 °C isotherm. For Hurricane Iselle, this may have been a key component of its trajectory parallel to the Hawaiian Islands, and subsequent landfall. In the case of Hurricane Julio, it is apparent that the storm tracked closely behind Iselle along the monthly mean 26 °C isotherm which was positioned to the northeast and north of Hawaii. A close inspection of oceanic conditions indicates that hurricanes can be sustained in the Eastern NPO with less than optimal oceanic conditions (i.e., when SST and/or UOHC are near the recognized minimum threshold of 26 °C). Although generation of these three hurricanes were observed to occur when SST, SSTA, UOHC, and UOHCA were higher than normal and well above established minimum thresholds, the maintenance of TCs does not appear to require the same level of surface layer temperatures as is characteristic in the Western NPO [16].

We also observed the emerging importance of oceanic conditions in the Central NPO through analyses of high SST and UOHC. In July and August 2014, the surface location of the 26 °C isotherm followed 30° N as far east as 155° W and to the north of the Hawaiian Islands. East of 140° W, we observed the 26 °C isotherm at the surface retreat to approximately 18–20° N as the influence of the much cooler California current and cool surface upwelling along the western U.S. coastline exerted dominant control over surface conditions. Positive SST anomalies were extant throughout the Central NPO, especially the southern and southwestern edge of the "Blob" around 30° N between 180° and 135° W. Our observed anomalies agree well with anomalies reported by Bond et al. [32] for February 2014, hinting at the long-lasting nature of this anomalous feature. Our analysis of Figures 2 and 3 point towards a strengthening of the southern portion of SSTA in the "Blob" in August of 2014.

The penetration of deep warm water from the West Pacific Warm Pool is also visible in both UOHC and UOHCA, and may have contributed to the final rapid intensification momentum of Hurricane Genevieve into the Western NPO. UOHC in this low tropical region exceeded 200 kJ cm^{-2}, with anomalies ranging from 20 to 80 kJ cm^{-2}, confirming the above-average potential available energy provided by the surface ocean during this hurricane season.

It is also important to discuss the El Niño conditions prior to the 2014 hurricane season. Indications of strong positive UOHC and SST anomalies in early 2014 pointed towards the development of a potent El Niño event, with initial similarities to the 1997–1998 El Niño [35]. However, the anticipated strong El Niño phase failed to initiate until the following year. While the 2014 NPO TC season saw above-average activity, prolonged UOHC and SST anomalies observed throughout the 2014 season persisted into 2015, and saw the genesis of record-breaking Hurricane Patricia in the Eastern NPO [36] during a positive El Niño event. Future research would benefit from additional case study analyses to further understand the linkages between upper ocean and SST anomalies as critical factors in the genesis and intensification of major TCs within the Eastern and Central NPO regions.

Supplementary Materials: The following are available online at http://www.mdpi.com/2077-1312/8/4/288/s1, Figure S1: Along-track SST for Hurricanes Genevieve, Iselle, and Julio at 0 to 5 days prior data extraction; Figure S2: Along-track depth of the 26 °C isotherm for Hurricanes Genevieve, Iselle, and Julio.

Author Contributions: Conceptualization, V.L.F. and N.D.W.; methodology, V.L.F. and N.D.W.; formal analysis, V.L.F. and N.D.W.; investigation, V.L.F., N.D.W., and I.-F.P.; data curation, I.-F.P.; writing—original draft preparation, V.L.F. and N.D.W.; writing—review and editing, V.L.F., N.D.W., and. I.-F.P.; visualization, V.L.F. All authors have read and agreed to the published version of the manuscript.

Funding: V.L.F. was funded by the Department of Oceanography and Coastal Sciences and the Earth Scan Laboratory, Louisiana State University, Baton Rouge, Louisiana. I.-F. P. is supported by Taiwan's Ministry of Science and Technology Grant MOST 107-2111-M-008-001-MY3.

Acknowledgments: Portions of this work were presented in thesis form in the fulfillment of the MS requirements for V.L.F. from Louisiana State University. V.L.F. thanks A. Haag of the Earth Scan Laboratory at Louisiana State University for their insight and programming assistance throughout this research study.

Conflicts of Interest: The authors declare no conflict of interest.

References

1. Rappaport, E. Fatalities in the United States from Atlantic Tropical Cyclones: New Data and Interpretation. *Bull. Amer. Meteor. Soc.* **2014**, *95*, 341–346. [CrossRef]
2. Berg, G.D. Eastern Pacific Hurricane Season. Technical Report; National Hurricane Center Annual Summary, 2015. Available online: https://www.nhc.noaa.gov/data/tcr/summary_epac_2014.pdf (accessed on 29 August 2015).
3. Bell, G.D.; Halpert, M.S.; Schnell, R.C.; Higgins, R.W.; Lawrimore, J.; Kousky, V.E.; Tinker, R.; Thiaw, W.; Chelliah, M.; Artusa, A. Climate assessment for 1999. *Bull. Amer. Meteor. Soc.* **2000**, *81*, S1–S50. [CrossRef]
4. Herring, S.C.; Hoerling, M.P.; Kossin, J.P.; Peterson, T.C.; Stott, P.A. Explaining Extreme Events of 2014 from a Climate Perspective. *Bull. Amer. Meteor. Soc.* **2015**, *96*, S1–S172. [CrossRef]
5. Businger, S.; Nogelmeier, M.P.; Chinn, P.W.; Schroeder, T. Hurricane with a History: Hawaiian Newspapers Illuminate an 1871 Storm. *Bull. Amer. Meteor. Soc.* **2018**, *99*, 137–147. [CrossRef]
6. Berg, R.; Kimberlain, T. The 2014 Eastern North Pacific Hurricane Season: A Very Active Season Brings Devastation. *Weatherwise* **2015**, *68*, 36–45. [CrossRef]
7. Leipper, D.; Volgenau, D. Hurricane Heat Potential of the Gulf of Mexico. *J. Phys. Oceanogr.* **1972**, *2*, 218–224. [CrossRef]
8. DeMaria, M.; Kaplan, J. Sea surface temperature and the maximum intensity of Atlantic tropical cyclones. *J. Climate* **1994**, *7*, 1325–1334. [CrossRef]
9. Whitney, L.; Hobgood, J. The relationship between sea surface temperature and maximum intensities of tropical cyclones in the eastern North Pacific. *J. Climate* **1997**, *10*, 2921–2930. [CrossRef]
10. Webster, P.; Holland, G.; Curry, J.; Chang, H.R. Changes in Tropical Cyclone Number, Duration, and Intensity in a Warming Environment. *Science* **2005**, *309*, 1844–1846. [CrossRef]
11. Goni, G.; Trinanes, J. Ocean thermal structure monitoring could aid in the intensity forecast of tropical cyclones. *EOS Trans. Am. Geophys. Union* **2003**, *83*, 573–578. [CrossRef]
12. Cione, J. The Relative Roles of the Ocean and Atmosphere as Revealed by Buoy Air-Sea Observations in Hurricanes. *Mon. Weather Rev.* **2015**, *143*, 904–913. [CrossRef]
13. Shay, L.; Goni, G.; Black, P. Effects of a warm oceanic feature on Hurricane Opal. *Mon. Weather Rev.* **2000**, *128*, 1366–1383. [CrossRef]
14. Mainelli, M.; DeMaria, M.; Shay, L.; Goni, G. Application of oceanic heat content estimation to operational forecasting of recent Atlantic category 5 hurricanes. *Weather Forecast.* **2008**, *23*, 3–16. [CrossRef]
15. Shay, L.; Brewster, J. Oceanic Heat Content Variability in the Eastern Pacific Ocean for Hurricane Intensity Forecasting. *Mon. Weather Rev.* **2010**, *138*, 2110–2131. [CrossRef]
16. Lin, I.I.; Pun, I.F.; Wu, C.C. Upper-Ocean Thermal Structure and the Western North Pacific Category 5 Typhoons. part II: Dependence on Translation Speed. *Mon. Weather Rev.* **2009**, *137*, 3744–3757. [CrossRef]
17. Fisher, E. Hurricanes and the Sea-Surface Temperature Field. *J. Meteor.* **1958**, *15*, 328–333. [CrossRef]
18. Price, J. Upper Ocean Response to a Hurricane. *J. Phys. Oceanogr.* **1981**, *11*, 153–174. [CrossRef]
19. Wroe, D.; Barnes, G. Inflow Layer Energetics of Hurricane Bonnie (1998) near Landfall. *Mon. Weather Rev.* **2003**, *131*, 1600–1612. [CrossRef]
20. Walker, N.; Leben, R.; Pilley, C.; Shannon, M.; Herndon, D.; Pun, I.F.; Lin, I.I.; Gentemann, C. Slow translation speed causes rapid collapse of northeast Pacific Hurricane Kenneth over cold core eddy. *Geophys. Res. Lett.* **2014**, *41*, 7595–7601. [CrossRef]

21. Gentemann, C.; Meissner, T.; Wentz, F. Accuracy of Satellite Sea Surface Temperatures at 7 and 11 GHz. *IEEE Trans. Geosci. Remote Sens.* **2010**, *48*, 1009–1018. [CrossRef]
22. Wentz, F.; Gentemann, C.; Smith, C.; Chelton, D. Satellite measurements of sea surface temperature through clouds. *Science* **2000**, *288*, 847–850. [CrossRef]
23. Ford, V.L. The Role of Upper Ocean Heat Content and Sea Surface Temperature on Northeast Pacific Hurricane Evolution During Average and Active Years. Master's Thesis, Louisiana State University, Baton Rouge, LA, USA, 2016.
24. Banzon, V.; Smith, T.; Chin, T.; Liu, C.; Hankins, W. A long-term record of blended satellite and In Situ sea-surface temperature for climate monitoring, modeling and environmental studies. *Earth Syst. Sci. Data* **2016**, *8*, 165–176. [CrossRef]
25. Xue, Y.; Smith, T.; Reynolds, R. Interdecadal Changes of 30-Yr SST Normals during 1871-2000. *J. Clim.* **2003**, *16*, 1601–1612. [CrossRef]
26. Pun, I.F.; Lin, I.I.; Ko, D. New generation of satellite-derived ocean thermal structure for the western North Pacific typhoon intensity forecasting. *Oceanography* **2014**, *121*, 109–124. [CrossRef]
27. Goni, G.; Kamholz, J.; Garzoli, S.; Olson, D. Dynamics of the Brazil-Malvinas Confluence based on inverted echo sounders and altimetry. *JGR Oceans* **1996**, *101*, 16273–16289. [CrossRef]
28. Pun, I.F.; Price, J.; Jayne, S. Satellite-Derived Ocean Thermal Structure for the North Atlantic Hurricane Season. *Mon. Weather Rev.* **2016**, *144*, 877–896. [CrossRef]
29. Landsea, C.; Franklin, J. Atlantic Hurricane Database Uncertainty and Presentation of a New Database Format. *Mon. Weather Rev.* **2013**, *141*, 3576–3592. [CrossRef]
30. Elsner, J.; Jagger, T. *Hurricane Climatology: A Modern Statistical Guide Using R*, 1st ed.; Oxford University Press: New York, NY, USA, 2013.
31. Farfan, L. Eastern Pacific Tropical Cyclones and Their Impact Over Western Mexico. In *Experimental and Theoretical Advances in Fluid Dynamics*; Klapp, J., Cros, A., Velasco Fuentes, O., Stern, C., Rodriguez Meza, M., Eds.; Springer: Berlin/Heidelberg, Germany, 2012; pp. 135–148.
32. Bond, N.; Cronin, M.; Freeland, H.; Mantua, N. Causes and impacts of the 2014 warm anomaly in the NE Pacific. *Geophys. Res. Lett.* **2015**, *42*, 3414–3420. [CrossRef]
33. Jin, F.F.; Boucheral, J.; Lin, I.I. Eastern Pacific tropical cyclones intensified by El Niño delivery of subsurface ocean heat. *Nature* **2014**, *516*, 82–85. [CrossRef]
34. Beven, J.; Birchard, T. Hurricane Genevieve (EP072014). Available online: https://www.nhc.noaa.gov/data/tcr/EP072014_Genevieve.pdf (accessed on 15 May 2016).
35. McPhaden, M. Playing hide and seek with El Niño. *Nat. Clim. Chang.* **2015**, *5*, 791–795. [CrossRef]
36. Foltz, G.; Balaguru, K. Prolonged El Niño conditions in 2014–2015 and the rapid intensification of Hurricane Patricia in the eastern Pacific. *Geophys. Res. Lett.* **2016**, *43*, 10347–10355. [CrossRef]